GEOTECHNICAL EVALUATION FOR EMBANKMENT USING GENERAL EQUILIBRIUM MODEL

***R. Galindo Muñoz*[1] *J. Montenegro Cooper*[2] *R. King St-Onge*[3]**

ABSTRACT:
This study is focused on a fill embankment located southeast of Tomé, a city in the VIII region of Chile. Place where this man-made earth structure complements a roadway. Finding the causes that led to the failure of the structure is the goal, to do this, information about the soils properties and geometry are needed. Laboratory tests will be carried out, such as particle-size distribution, plasticity limits, modified Proctor tests and also direct shear resistance tests. The final step is to generate a model with properties and the Geometry of the embankment. SLOPE/W is the tool that will assist in the process. It will assist in solving the shear and normal force balances that act over the embankment. Different resistant conditions for the embankment will be analyzed. General limit equilibrium analysis method will be applied. With this method safety factors can be found for resistant parameters where the structure would probably fail.

RESUMEN:
El presente estudio se enfoca en un terraplén localizado al sur este de Tomé, una ciudad de la VIII región de Chile. Lugar en donde la estructura artificial de suelo complementa una calzada. El objetivo es encontrar las causas por las cuales está fallando, para esto, información de las propiedades del suelos y geometría de la estructura son necesarias. Ensayos de laboratorio serán llevados a cabo, tales como granulometría, límites de Atterberg, Proctor modificado, corte directo, entre otros. Con la información recopilada se generó un modelo digital del terraplén con sus propiedades y dimensiones. SLOPE/W es una herramienta que asistirá durante el proceso. Se utilizará para resolver el balance entre las fuerzas normales y de corte, que actúan sobre el terraplén. Se analizaron distintas condiciones de resistencias y se aplicará el método general de equilibrio limite. Los factores de seguridad para el momento de falla fueron calculados al final del análisis.

[1] Student, Civil Engineering Career, Catholic University of the most Holy Conception, CHILE, rigalindo@ing.ucsc.cl
[2] Guide Professor, Civil engineering department, Catholic University of the most Holy Conception, CHILE, jmontenegro@ucsc.cl
[3] Informant Professor, Civil engineering department, Catholic University of the most Holy Conception, CHILE, rking@ucsc.cl

1 INTRODUCTION

The constant growth and progress of a country have a direct relation with the increase of territorial occupation. Land can be used for several purposes, such as industrial, housing areas, or touristic attractions. Concrete or asphalt roads can be built to establish a solid connection between locations. Soil structures are necessary when the required path has to surround a steep slope or go through natural terrain. The elevation of an existing ground level can be done using embankments, to satisfy the requirements of a specific road design (Moldovan, Nagy, Muntean, & Ciotlaus, 2017). Embankments can sustain roads or other constructions if they are well constructed; a poorly made structure will have lower resistance to shear forces and ground water pressure. Slope instability is a problem found in geotechnical engineering, and it can potentially cause major losses of properties and even life (Chok, 2008). All the conditions that surround the construction of an embankment must be studied for its optimal performance. In this work, an embankment failure has been studied to understand what elements are involved and how harmful can they be.

1.1 Investigation and location description

This paper studies an embankment located southeast of the Chilean city named Tomé. The exact location is over the O-300 route at the 2.1 km mark between Tomé and a small village, El Laurel. The O-300 is mainly a dirt road but paving works have taken place over different sections of this path. Eventually cracks were produced over the pavement after a period of time at a specific curve. Further observation determined that the cause was an embankment failure sustaining the pavement.

Soils of the study zone are composed in a great portion of weathered granite. Decomposition of minerals in this zone is relatively normal due to the climate factor. The conditions or rain and wind mixed with high temperature in the summer makes the decomposition proceed over some minerals found in the area. Figure 1 (a) displays the study zone with different soils and minerals that are located around the area of study, also the legend for each colored zone.

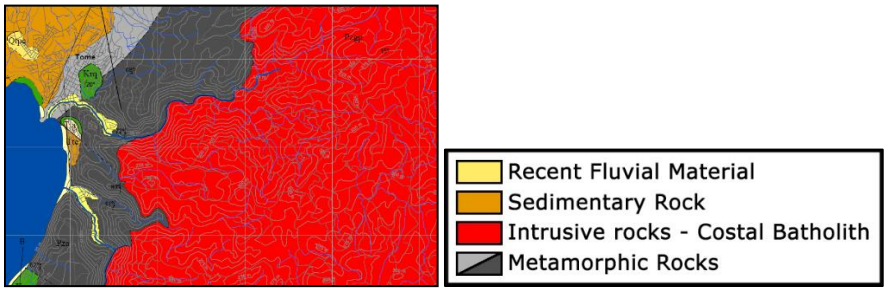

Figure 1: Geologic map of area of study with associated legend (modified from Gallardo, 1981)

In Chile one of the most frequently found soils produces by the weathering of granite rocks is a residual soil locally known as “maciillo”. This soil has a complex composition that makes it difficult to define its mechanical properties as a withered rock or a soil or even a mixture of both. The soils behavior can affect the stability of fill slopes and embankments or any kind of construction that is built over. (Rodriguez, 2015)

1.2 Design and construction of Embankment

Ruiz (2007) indicate that embankments are a human-made ground modification that increases the natural soil profile. The main parts of an embankment are: foundation, toe, facing, crest, and slope angle (Han, 2015), these parts are displayed in Figure 2. The author mentioned above defines each part the embankment as follows:

- Foundation: Soil below the original surface of the land. Inappropriate materials need to be removed or improved.
- Nucleus: This is the embankments core located between the foundation and the coronation. Most of the soil volume of the embankment is here.

- Facing: Side and outer part of the embankment, usually formed according to the slope angle.
- Crest: Upper layer where the sub-base is settled.
- Slope angle: Angle measured from a horizontal plane at a given point of the land surface to ensure facing stability.

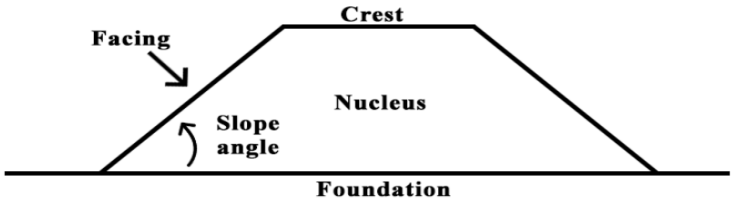

Figure 2: Parts of an embankment

Embankment construction requires good quality surrounding material as much as an optimal foundation with reliable geotechnical properties. Several national and international standards (Ministerio de foment, 2002; MOP, 2002; Geotechnical engineering BUREAU, 2015; Washington state department of transportation, 2013), as well as scientific articles (Oteo, 2011; Ministry of transportation Ontario, 2016), proposed design methods for earthworks. In Chilean public works should use the Manual de Carreteras, volume III for design and volume V for the construction process, published by the Public Work Ministry (MOP).

In general, most codes agree to request similar technical requirements. Technical earthwork aspects can be divided into two categories: design and construction. Design recommendations depend on the knowledge of the available materials near the construction site (Gonzalez Vallejos et al., 2004). Indeed, the design of a slope should be adjustable to the available materials and the requirements of technical specifications. It is important to state that depending on the specific standard used, the design may change. Compaction and drainage are the most important issues that should be considered (Gonzalez Vallejos et al., 2004).

On the other hand, quality control of every step in the embankment construction (foundations, every compacted layer, drainage system, slope angle, etc.) needs to be checked. Several laboratory and in-situ geotechnical tests (Modified Proctor, CBR, dry density and moisture, plate test, in situ CBR, etc.) can be performed to ensure that the work has been accomplish correctly. In case of a large extension of earthworks, to improve the construction process a test court can be made to achieve the best method with available machinery (Aguas andinas, 2011).

The quality control of every single soil layer is performed with the “finished product control” method. Two conditions have to be achieved for an acceptable layer compaction:

- Dry density and compaction moisture is above the minimum established by the construction project or the construction manager. Also, the degree of saturation needs to be between the limit established by the country code.
- The vertical module of deformation performed with a load plate test (E_{V2}) is the minimum according to the NLT 357 standard. Each embankment part requires a different value range for E_{V2} (Spanisch Standard, PG3)

Independent of the design and construction controls, several earthworks in different roads and tracks have been failed every year. In general, Han (2015) found that four different types of failures can occur (see Figure 3): i) global failure, ii) toe slope, iii) superficial and iv) local. The most common failure is the surficial failure, it can be caused by several reasons: poor compaction, low overburden stress, loss of cohesion, etc. (Han, 2015). Each failure type utilizes a specific volume of soil that moves. For example, a global failure will cause the most destructive damage, while the local is the smallest and simplest to repair.

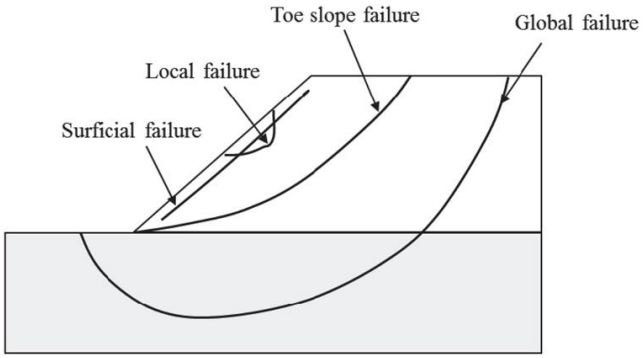

Figure 3: Potential slope embankments modes (Han, 2015)

The Federal Highway Association (FHWA) is an agency within the U.S. Department of Transportation that supports State and local governments in the design, construction, and maintenance of the Nation's highway system (Federal Aid Highway Program) and various federally and tribal-owned lands (Federal Lands Highway Program) (US. Department of transportation, 2019). Embankments that are placed over weak foundations vulnerable to instability problems, there are 4 types that should be considered These are displayed in figure 4 (FHWA, 2001).

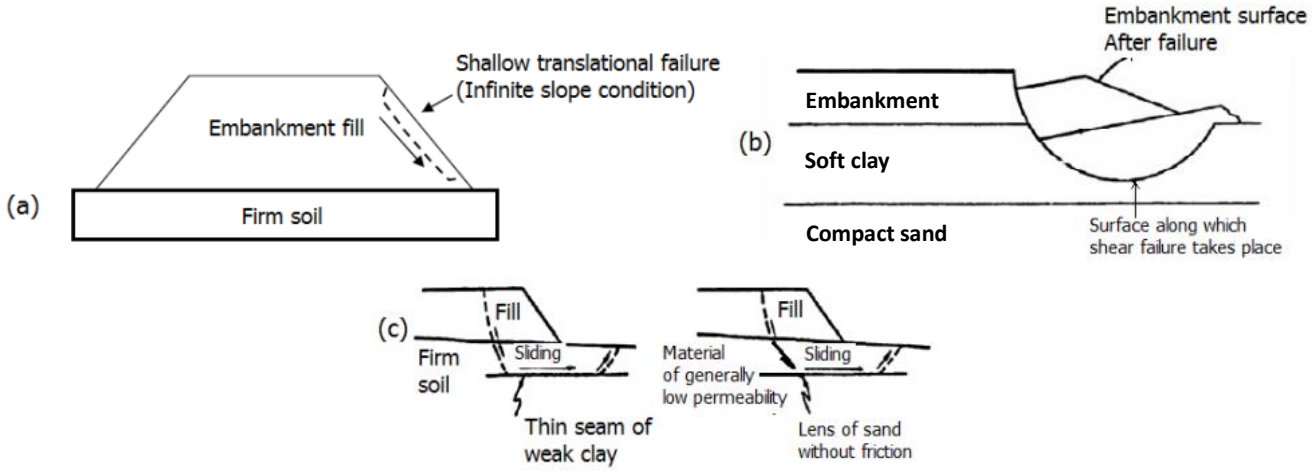

Figure 4: Typical embankment failures: (a) Infinite slope, (b) circular, and (c) Sliding block (FHWA, 2001)

1.3 Slope stability

The slope stability of embankments or any other earthworks and natural slopes are governed by the shear strength of soils. The usual model used to predict shear resistance is the Mohr-Coulomb (see equation 1). Two soil parameters need to be defined in the laboratory or in-situ to use the aforementioned model. The shear strength of the soil (τ) depends on three soil parameters angle of internal friction ($\emptyset$), cohesion (c) and the effective stresses (σ'_n) applied in the failure plane.

$$\tau = c + \sigma'_n \cdot tg\emptyset \qquad (1)$$

The angle that forms the linear regression with the horizontal is the angle of internal friction ($\emptyset$), and where the regression touches the ordinate axis is the cohesion. Both geotechnical parameters have to be determined by the laboratory, or in-situ tests. Figure 5 shows the Mohr-Coulomb failure envelope with every parameter (GEO-SLOPE International, 2012).

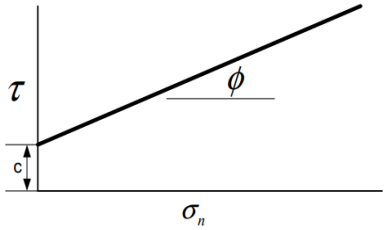

Figure 5: Representation of Coulomb shear strength equation.

The stability of slopes is studied, taking into account the general limit equilibrium (GLE) methods. The certain equilibrium of the mass could be achieved if the three equations of the static are fulfilled. Equilibrium, in physics, is the condition of a system where neither of the states of motion nor its internal energy state is changing through time. Two of those equations assure the null movement of the mass in any directions (both equations assure each perpendicular directions), while the third, guarantees that the mass does not rotate. Figure 6 shows a theoretical slice of mass from an embankment displaying the forces to which it is subjected.

Several procedures to solve the problem have been proposed. Some of the models evaluate the complete sliding mass (ordinary Fellenius), while others divided the sliding mass into several slices (Bishop's simplified, Janbu's simplified, Spencer, Morgensten-Price, among others). The useful simplification that produces the division of the whole mass into slices that also cause that loads applied is distributed on each slice of the sliding mass. Each slice is affected by internal and external forces. The method of slices is used in most computer programs.

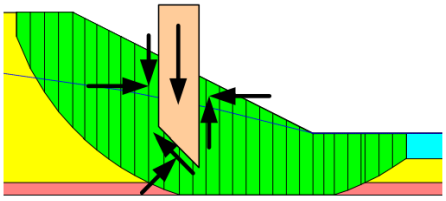

Figure 6: Circular slip surface and slice forces on a sliding mass

To establish the stability of a soil mass the safety factor (FOS) must be determined. It can be done by comparing the forces that tend to produce a slip with the forces that are trying to avoid a slip (Valiente, 2015) (see equation 2). The potential failure of the slope has to be studied determining the factor of safety of the slope, taking into account the geological, hydrogeological, and geotechnical model. The proposed model (soil or rock stratigraphy, water level, natural density of materials, earthquake effects, etc.) has to consider the worst case that could occur. The geotechnical model needs to be done according to the previous background, field and laboratory tests, monitoring, and site visits, among others.

$$\text{FOS} = \frac{\sum Resisting\ forces}{\sum Sliding\ forces} \qquad (2)$$

The main difference between the previously mentioned models is the number of equilibrium equations that these models satisfy. The number of slices required to determine the factor of safety of slopes depend on some embankment attributes (height, slope angle, drainage conditions, accuracy required, etc.) and is also related to the number of equations. Solving the mathematical problem requires an equal number of equations and unknown factors. In general, this kind of problem will mostly present a greater amount of unknowns.

Every model can be differenced according to the forces that each one takes into account. Figure 7 a) y b) shows forces considered in each slice by Fellenius and Spencer methods, respectively. Fellenius method considers only

the moment equilibrium, with no regard to the equilibrium of forces. On the other hand, Spencer method considers both force directions (X and Y) and the moment equilibrium.

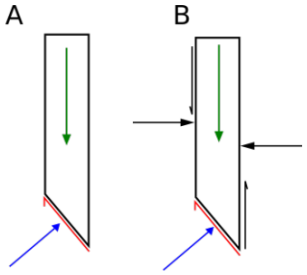

Figure 7: Free body of the following methods: a) Fellinius b) Spencer (Hernvall, 2017)

Since the existence of the ordinary method of slices, more methods have been developed for equilibrium limit analysis. Slope analyses using different methods will not have the same factor of safety.

Figure 8 shows the free body diagram of one slice. The principal forces of each slice are the weight (W), normal and shear reactions among the slice and the soil (E and X). Two types of normal and shear forces are presented in the image: inter-slices (sides of the slice) and between the slice and low part of the soil mass (low side of the slice).

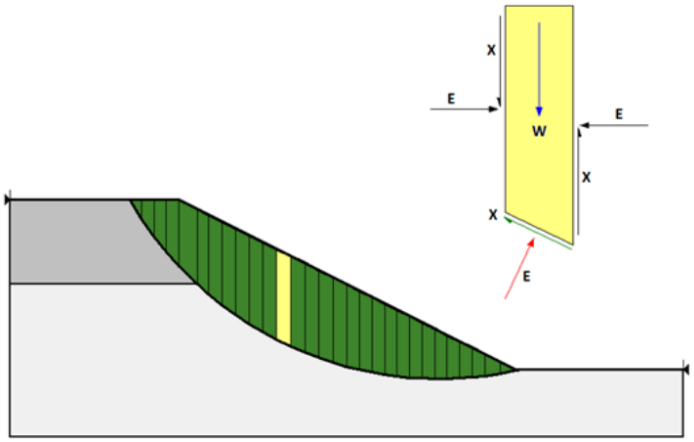

Figure 8: Circular slip surfaces and the interslice forces of a selected slice together with a free body diagram (GUSTAFSSON & LINDSTROM, 2014)

Some methods of analyses consider the X equilibrium of forces to determine the safety factor and consider inter-slice forces between slices. According to the method, the inter-slices forces (E) are functions f(x) and a percentage used of that function is **λ**, such as can be seen in Equation 3. For example, Spencer method considers the function constant along all the inter-slices forces, while Morgentsen–Price proposed a function among the inter-slices. The quantity of the specific function will vary along the slices, and the angle of the resultant shear force will be obtained by arctan (X/100). Figure 9 displays how the function contribution by **λ** will vary along with every slice through a half-sin function.

$$X = E\,\lambda\,f(x) \qquad (3)$$

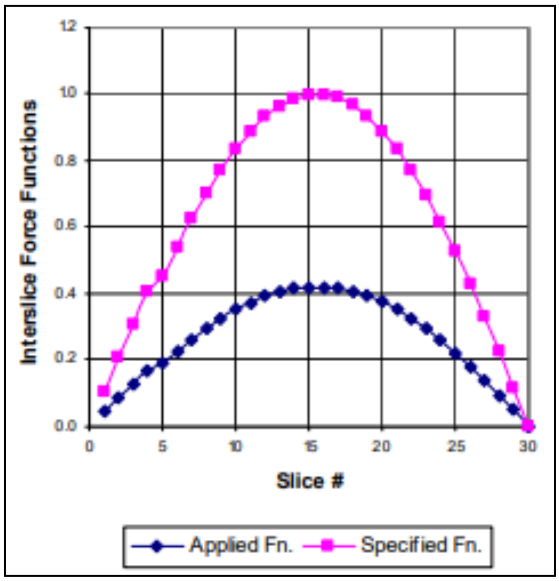

Figure 9: Half sin inter-slice force function **(GEO-SLOPE International, 2012)**

The factor of safety could be determined with non-rigorous and rigorous models. The difference between both is the fact that in the first only parts of the equilibrium equations are fulfilled, although in the second all equilibrium conditions are satisfied. Table 1 shows the equilibrium equations fulfilled by each model. Rigorous models are those where the forces (x and y) and moment equilibrium are fulfilled, such as Spencer, Bishop's generalized, Sarma, and Morgentsen-Price.

Table 1: Equations of Statics Satisfied (Abramson et al., 2001)

Method	Force Equilibrium		Moment equilibrium
	X	Y	
Ordinary or Fellenius	No	No	Yes
Bishop's simplified	Yes	No	Yes
Janbu's simplified	Yes	Yes	No
Lowe-Karafiath	Yes	Yes	No
Corps of Engineers	Yes	Yes	No
Spencer	Yes	Yes	Yes
Bishop's generalized	Yes	Yes	Yes
Janbu's generalized	Yes	Yes	No
Sarma – vertical slices	Yes	Yes	Yes
Morgenstern-Price	Yes	Yes	Yes

Slope failures occur when the soil resistance is overtaken by internal forces, as a consequence of internal or external forces applied. The slopes' failure occurs as a movement of the soil mass or its rotation. The failure occurs when the factor of safety is equal to one, i.e., shear resistance and sliding forces are in a state of limit equilibrium.

The factor of safety required in earthworks depends on the code or standard used in the design process. Chilean standard commonly requests -considering the earthquake effects- safety factors above 1,2, that means that shear resistance is 20% higher than the most extreme load hypothesis (considering earthquake effects) that develops the sliding mass.

In the case of embankment constructions over soft soils or steep slopes, that need to be improved, due to the factor of safety below de correspondence standard, reinforcement techniques have to be utilized. Several techniques are developed to improve the sliding mass, such as geosynthetic reinforcements, piles, anchors, soil nailing, stone columns, geopier, vertical drains, jet-grouting, among others (Han, 2015). Several authors classified the ground and soil improvement (Mitchel, 1981; Hausmann, 1990; Ye et al., 1994; Scaefer and Berg, 2012). Han (2015) classified the ground improvement according its function, such as i) densification, ii) replacement, iii) drainage, dewatering, and consolidation, iv) chemical stabilizations, v) reinforcement, vi) thermal and biological treatment. According to the aim of the enhancement, the appropriate technique is chosen.

1.4 Shear strength resistance

Any engineering project will transmit stress forces to the soil underneath, besides the own ground weight. Although the soil can have failures due to great applications of compression stress, but generally the soil fails by shearing forces. When the surface of the soil is inclined, such as embankments, a shear stress will be generated. If the sliding force surpasses the shear soil resistance the structure will fail. Figure 10 displays how a soil might behave when there are shear forces applied. A soil can act as a fragile or ductile material, its deformation curve is non-lineal and plastic at first, there is no rupture point.

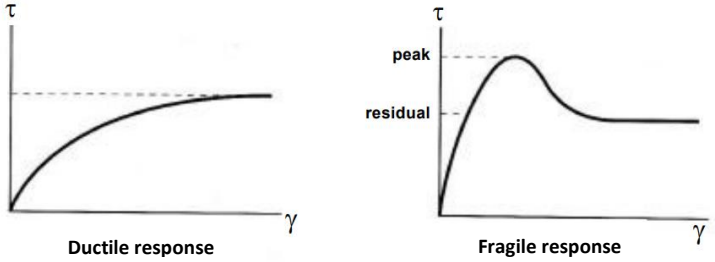

Figure 10: Different resistance response between ductile and fragile soil

When a soil has a fragile behavior it presents a peak resistance and finally a residual resistance at higher values of shear stress. In sand type soils the resistance between a dense and loos condition should match at the end of a shear stress test.

1.5 Superficial wave analysis

The shear modulus is the response from the earth's material to the shear deformation (Sanjeev, 2016). It is a critical engineering parameters and is directly related to the soil stiffness. In seismic studies the shear velocity (Vs) is the best soil stiffness indicator. There are several methods for studying Vs, some are not profitable due to field operations, data analysis and overall costs. The MASW (Multi-channel Analysis of Surface Waves) is a seismic survey method to study de elastic condition of the subsurface for geotechnical purposes (Abdullah, 2012). Using MASW, shear-wave velocity (Vs) variations below the surveyed area can be recorded and analyzed. Figure 11 displays the resulting image of a MASW test with variation of Vs and the range of depth and longitude used.

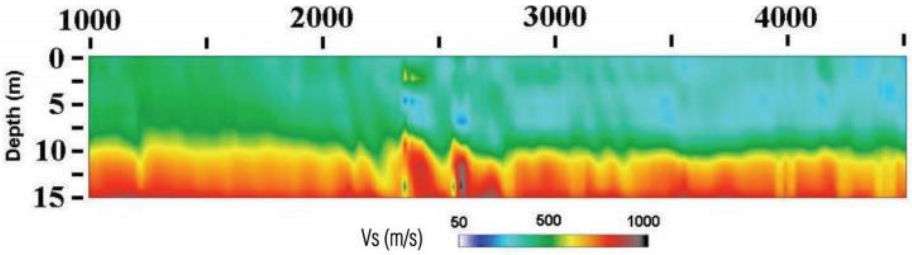

Figure 11: Resulting image of a MASW test (Choon, 2007)

A specific software must be implemented to read and process all the data obtained by the receptors. Vibrations from surface waves are the main source of data, they can be generated naturally or manually using, for example, a sledge hammer. Shear-wave velocity can be deduced and its variation through the soil layers beneath the surface. Salem (2016) Mentions that "After the February 27th, 2010 Maule Chile Earthquake, the National Chilean standard for seismic design of buildings (NCh 433 of.96 mod. 2009) underwent a series of modifications. One such modification was in regards to seismic soil classification" (pág. 16).
In Chile this classification must be carried out for any kind of structures due to the seismic activity present in our country, this will establish the quality of the soil and also the additional information that is required. The parameter Vs30 is needed now and is calculated as:

$$V_{s30} = \frac{\sum_{i=1}^{n} h_i}{\sum_{i=1}^{n} \frac{h_i}{V_{s-i}}} \qquad \textbf{(10)}$$

Where:
V_{s-i}: Shear wave velocity of stratum i, in m/s
h_i: Width of stratum i, in m
n: Number of stratum in the superior 30 meters of the terrain
(MINISTRY OF HOUSING AND URBANISM, 2011)

2 METHODOLOGY

The present investigation describes the process to elaborate a diagnosis for an embankment failure. Soil information has been gathered through various test on field and laboratory tests performed at the catholic university of the most holy Concepcion (UCSC) laboratory. A field visit was carried out to evaluate the study zone and collect samples for every necessary test. The laboratory tests involved were necessary to characterize the material and obtain the characteristics, index properties and resistance strength, among other information. This article explains further on, in more detail, every test done. This section also includes geophysical and topographic tests that add additional information related to the embankments geometry and geophysical details. All the equipment was provided from the UCSC laboratory. The information acquired has led to the creation of a general equilibrium limit model (GLE).

The methodology has been divided in three sections (Laboratory tests, Field Tests, GLE model), explaining in detail every procedure in a summarized manner. The information is not displayed in a chronological order.

2.1 Laboratory

All the actions that took place in the UCSC laboratory are considered in this sub chapter. The tests that are considered are the following; particle distribution, Atterberg limits, Modified Proctor, particle density and shear resistance. Every test has been carried out in regards to their respective standard used in Chile. It should be mentioned that there are two samples from different soil samples, the first is directly from the embankment (Soil M1) and the second was extracted from the surrounding area of the embankment (Soil M2).

2.1.1 Soil classification

Studying such a complex material such as soil, requires a methodology and an evaluation system than can be understood by different professionals around the world. The four big groups where soils can be classified are gravel, sand, silt and clay.

A mass of soil can contain a portion of each one of these groups and to quantify the proportion a particle size distribution can be done. To perform this test adequately, in Chile, it must follow the procedure established in "*Manual de carreteras - Especificaciones y métodos de muestreo, ensaye y control"* (Dirección de Vialidad, 2010). For this investigation the sieve configuration was obtained from "*Curso Laboratorista Vial Clase C"* (Jeria H., 2018), Table 2. The quantity of material used depends on the samples maximum particle size, therefore 0.5kg was

taken from each sample. The finer material was washed off thoroughly from both samples separately. There was only tap water available for the washing process. After eliminating all of the finer material, the soil was dried out. After every change in the soil, weight would be registered. After the soil is prepared the sieving stage takes place using the following configuration (Sieves with larger openings did not retain any material):

Table 2: Particle distribution sieves (Jeria H., 2018)

Nominal sizes of openings	
mm	ASTM
2.5	N°8
2	N°10
1.25	N°16
0.63	N°30
0.315	N°50
0.16	N°100
0.08	N°200

As usual in this test, the retained soil weights of each sieve was registered and the percentage of passing soil was calculated for each sieve size. Some extrapolation was necessary for other sizes not included in this configuration.

A liquid limit test follows the NCh1517/1 of 1979 standard as a guideline. The procedure was done 6 times for both soils (M1 and M2). Equipment such as a liquid limit device, watering bottles, and a grooving tool were provided by the laboratory. The liquid limit device has a metal cup where about 100g of soil fits to make a circular mold, with different values of moisture. The grooving tool made an incision cutting the mold in half, creating an opening. Then the cup was lifted and dropped until the gap is only 10mm wide. For every test the moisture content and amount of drops were recorded.

For the Plastic limit (PL) the NCh1517/2 of 1979 standard was used. This test consists in finding the soils moisture content where the material begins to crumble. Using evaporating dishes and a watering bottle the test was carried out three times for each sample. The samples at different moisture contents were rolled up into threads about 3mm in diameter, every time this was done the weights were recorded to obtain further on the moisture content.

The NCh1532.Of80 standard is used to carry out a particle density test. Using a normalized density bottle and a small amount of soil. Inside the bottle the soil was placed and barely drowned in water, every material had its weight recorded. Using a vacuum pump for approximately 8 minutes, the air was completely extracted from the soil. A specific water temperature of 20°C is required to record the final weight of the sample. the laboratory oven was used to regulate the temperature.

2.1.2 Modified proctor

The standard for this test in Chile is the NCh1534/2 of 2008. The samples were sieved with ASTM N°4 (Method A) to have a uniform representative material and eliminate fewer oversized particles. Both samples were tested five times with different moisture contents. The soil was then placed in layers inside the metallic mold where the 4.5kg load is dropped 25 times per layer. A soils mold was extracted every test from where the moisture content would be obtained.

2.1.3 Shear stress

Both soil samples were submitted to this test. The M1 soil sample extracted directly from the embankment is the main focus. Oversized particles were eliminated by sieving, obtaining a representative sample. Usually this test is

carried out using undisturbed samples that represent the natural state of the soil. In this case, the embankment material was loose and soft, it was not possible to obtain undisturbed samples. The goal was to obtain the residual strength from a re-molded sample.
Every specimen of this test was remolded to an 80% of the MDD density (modified proctor test). The procedure for this experiment is under consolidated and undrained conditions. A saturated state of the soil is forced to recreate an unfavorable scenario. Due to the fact that the soil has a considerable concentration of fine particles, this process lasted 24 hrs.
After the sample is saturated, each one will go through a 12hr loading stage to complete the consolidation phase. There was one specimen for each level of vertical stress: 50 kPa, 150kPa and 300 kPa. The direct shear equipment has 2 separate parts that hold the soil mold (figure 12). A cut is produced with a horizontal movement of the lower half. This will result in a shear resistance produces between the upper and lower halves of the soil. The machine can run in both directions, forward or backward.

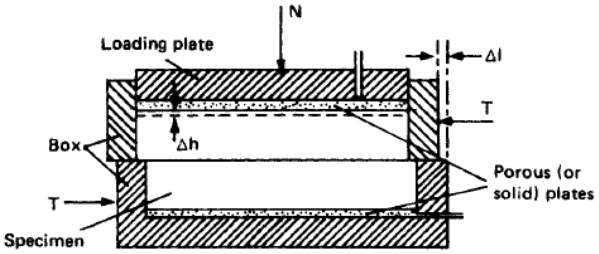

Figure 12: Direct Shear apparatus. (F. Craig, 2004)

When the consolidation concludes, specimens went through 3 motions of cutting. The first shearing motion forward, a second movement in the opposite direction returning to the initial position and finally a second shearing motion. Every test was configured to run at extremely low speeds for the undrain condition. Groundwater pressures were avoided using slower movement speeds. Only the soil resisted the shear stress generated by the equipment. All the results are summarized in the results chapter, the increment of shear strength is visible as the vertical load increases, until the point where the material fails. The test generated shear strength vs deformation graphs.

2.2 Field tests

The actions that take place at the investigation site are explained in this section, such as, topographic and geophysical tests. Also, it's also necessary to mention the site visit, soil sample extraction and field evaluation. This stage required manpower and equipment transportation.

2.2.1 Site visiting and sample extraction

Several trips were required for this investigation. The first visit was mainly to review the embankment and the surroundings. Figure 13 shows the embankments crest and the state in which it was found. There were some observations made during that day: Cracks over the pavement; Loose soil that was sliding downhill; Plants and trees with shifted location; upper soil layer contaminated with concrete and gravel.

Figure 13: First field visit, lateral view of the slope, detachment from the pavement

The goal of the second visit was to obtain soils samples. There are two extraction points for the samples: natural soil over the surrounding area and the material implemented on the embankment construction. The soil was stored in plastic bags and afterwards went through mixing process to obtain a uniform sample. Figure 14 displays how the samples were stored and labeled.

Figure 14: Samples that were stored in plastic bags to avoid moisture loss

2.2.2 Topography

This test a required a total station with a prism pole for measurements. To simplify the execution of this test a radial survey method was used. The total station was placed in a static location with one operator that would aim the equipment and record the coordinates of every point. Meanwhile a second operator will position the prism pole in different location over the embankment. Coordinates where processed after to generate a slope and elevation model of the embankment.

2.2.3 Geophysical

Geophysical information was obtained from the subsurface in this study using a multichannel analysis of surface waves (MASW) method. The equipment receptors were buried under the embankments surface each one separated 1m from each other. For this specific test there were two lines of receptors, transversal to the embankment and the second along the top longitudinally, figure 15 shows the longitudinal receptor positioning. There were 3 positions where a sledge hammer was used to hit a metal plate over each line, at the end of the line, the middle and at the beginning. A computer with the adequate software is where all the data was recorded from every hit. Finally, the data was processed through “SiesImager” a software that can analyze the MASW data and generate an image to observe the variations of the Shear-wave velocity beneath the soil in its different layers.

Figure 15: Latitudinal position of receptors along the embankment crest

2.3 GLE modeling

For the following part of this investigation, the software Slope/W was implemented. The software works with shapes and materials to specify different types of embankments and soils. Geometry and stability properties of the structure were obtained through the laboratory and Insitu tests. The goal was to obtain a factor safety that will satisfy the limit state of resistance, where its value is equal to 1.0. This was acomplished changing the values of cohesion and the internal friction angle. Many pair of values for thees soil properties can be found to achieve a factor equal to 1. There is another variable than can alter the result in this process, that is the Phreatic level. There will be 3 chosen freatic levels proposed for this specific problem displayed in figure 16

In the following model, weight of the concrete road over the embankment has be considered. The specific weight of concrete can vary from 2.35 kN/m3 to 25 kN/m3, depending on the type of materials that were during the construction. On this research the weight value used for the concrete road was 2.4 kn/m3 for the 6m length of the road that was measured.

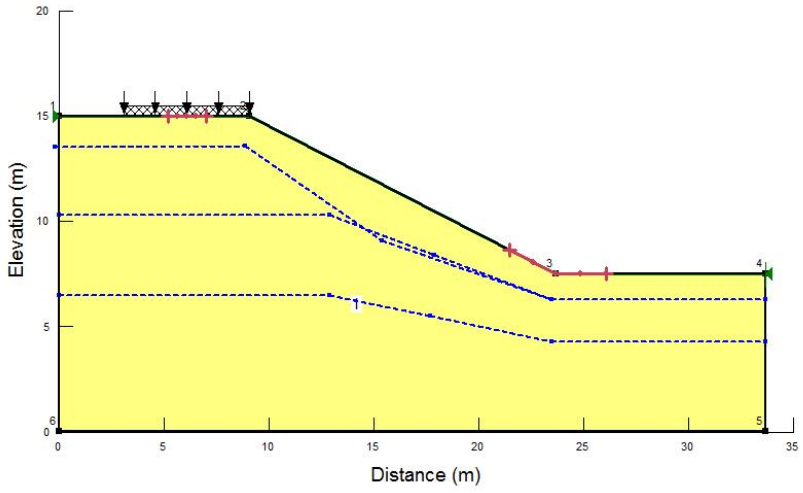

Figure 16: GLE model With a high Phreatic level (generated manually)

With this starting model, the position of the Phreatic level was changed maintaining a weight unit of the soil as 15 kN/m3. The resulting slop surface would be generated as shown in figure 17:

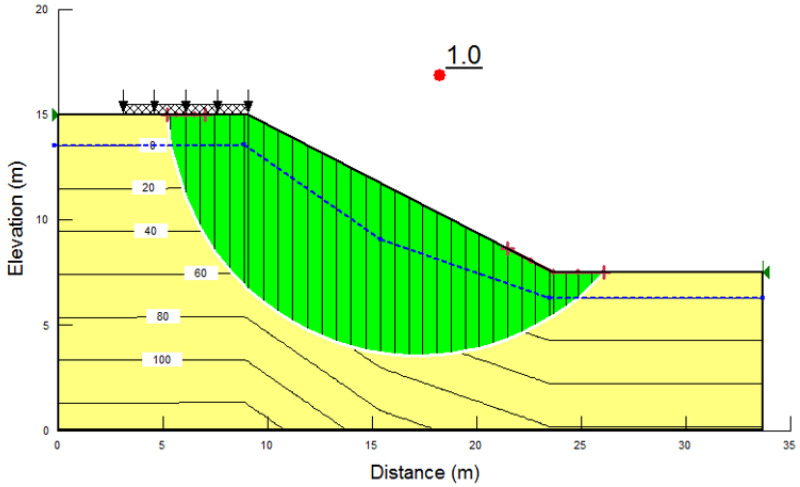

Figure 17: Slip surface with FoS =1

3 RESULTS

The results are divided in sections to maintain an order in this article; laboratory tests, Field Tests and GLE modeling.

3.1 Laboratory

The laboratory tests carried out in the Geotechnical Laboratory of the University of the most Holy Concepcion. Tests are divided in soil classification, followed by results for the direct shear tests.

3.1.1 Soil classification

The characterization of the soil required first the classification of each sample (M1 and M2). Table 3 displays the weight tabulation required to obtain the amount of fine material present in both samples. Equation 11 is the form in which the passing soil percent through the N°200 sieve is calculated.

Table 3: Test weights for the percentage of fine material

	M1 Soil	M2 Soil
bowl weight [g]	166	204.2
bowl + dry soil [g]	551.3	600.6
bowl + dry washed soil [g]	357.6	336

$$N°200\ sieve\% = \frac{Dry\ Soil\ Weight - Dry\ Washed\ Soil\ Weight}{Dry\ Soil\ Weight} \quad \textbf{(11)}$$

$$N°200\ sieve\%\ (M1) = \frac{385.3 - 191.6}{385.3} = 0.503 \approx 50\%$$

$$N°200\ sieve\%\ (M2) = \frac{396.4 - 131.8}{396.4} = 0.668 \approx 67\%$$

Having over 50% of fine soil, both samples can be classified as fine grained soils according to the unified classification system (USCS) (ASTM D2487-11). The considerable amount of fine particles indicates that the soils

present a low permeability and draining rate. The presence of water produces swelling over this type of soil that will affect the stability of structures such as embankments.

The grain size distribution is displayed on figure 18, the sieve configuration mentioned on index 2.1.1.

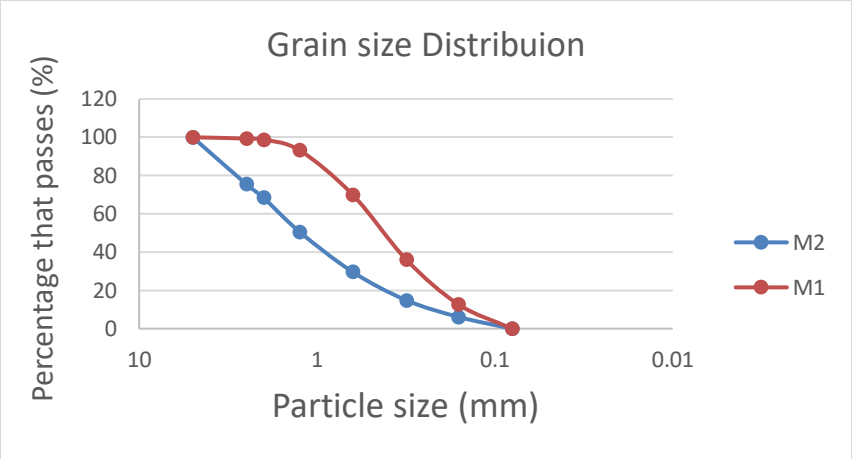

Figure 18: Particle distribution for soils M1 and M2

A point-line graph is used for the particle distribution curve. Soil M1 presents a gap for larger particles between 5mm and 2mm but both samples are well graded.

When studying fine-grained soils, the Cassagrande plasticity chart displayed on figure 19 can be used in parallel with the Atterberg Limit tests to distinguish basic soil types.

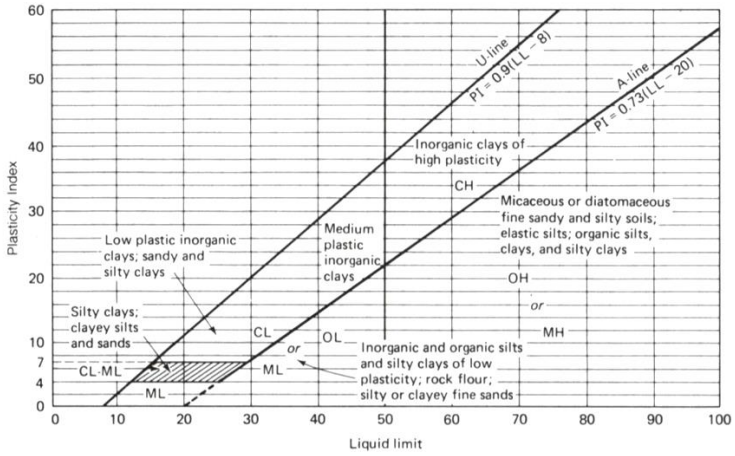

Figure 19: Basic types of soils that are represented on the Cassagrande plasticity chart (Holtz and Kovacs, 1981)

Figure 20 displays the results for the liquid limit (LL) test using the Casagrande method. The results of the liquid and plastic limit tests are summarized on table 4. Both samples can be considered soils of low plasticity having a LL lower than 50% and M1 requires a lower amount of water to change its behavior between a solid, plastic or liquid soil state. Which means a higher chance of it becoming unstable due to the increase of rain water during the winter season.

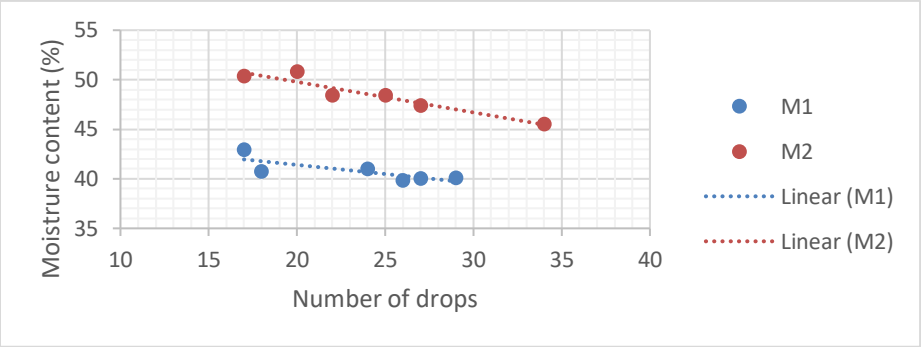

Figure 20: Liquid limit test results

Table 4: Limits and plasticity index,

	M1	M2
LL (%)	40.5	48.2
PL (%)	33.9	37.65
PI (%)	6.49	10.59

Now it's possible to identify each soil with the procedures of classification stated by the USCS. using the results obtained previously in conjunction with the information presented on table 5, a basic soil classification is done.

Table 5: Classification results using USCS and Cassagrande

Soil	M1	M2
PI on A line	14.96	20.58
Position	Below line A	Below line A
Classification	ML	ML

The conclusion is that both samples, on the Cassagrande chart, belong the inorganic or organic silts of low plasticity.

3.1.2 Modified proctor and Direct shear test

To carry out the direct shear test, as mentioned before in this article, it is convenient to have an undisturbed sample of soil than can be carved into the mold. In this case the only way to do this test is with a remolded sample to a to a maximum dry density (MDD). Figure 21 displays the outcome of the modified proctor test that has been completed for each soil sample. On table 6 the results show that both samples are capable to reach around the same value of maximum density. The difference is the amount of water each soil needs, sample M1 requires less moisture content in this case.

After the modified proctor test concludes and the data has been registered, a direct shear test can take place using the previous results. As mentioned before the mold we be remolded to a certain value of density established by the proctor test. under normal work conditions it is not possible to obtain the maximum density, that is why in this test it has been established that the sample will be remolded to an 80% of its densest condition.

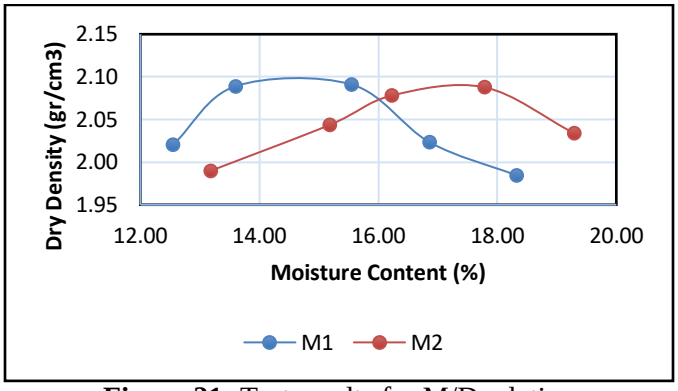

Figure 21: Test results for M/D relation

Table 6: Values of maximum dry density and its requiered moisture content

	Sample M1	Sample M2
opt. Moisture [%]	14.55	17.4
Max. Dry density [gr/cm3]	2.1	2.09

The direct shear equipment will be used to fin d the residual resistance through stages of backward and forward motions to cut the sample twice. All the stages are summarized in table 7 with its respective vertical load. To simplify any reference to any of the tests in this section each stage is assigned a test code.

Table 7: Shear test abbreviation and description

Test	Soil Sample	Vertical load (kPa)	Motion	Test	Soil Sample	Vertical load (kPa)	Motion
1.1-a	M1	50	Forward 1	2.1-a	M2	50	Forward 1
1.1-b	M1	50	Backwards 1	2.1-b	M2	50	Backwards 1
1.1-c	M1	50	Forward 2	2.1-c	M2	50	Forward 2
1.2-a	M1	150	Forward 1	2.2-a	M2	150	Forward 1
1.2-b	M1	150	Backwards 1	2.2-b	M2	150	Backwards 1
1.2-c	M1	150	Forward 2	2.2-c	M2	150	Forward 2
1.3-a	M1	300	Forward 1	2.3-a	M2	300	Forward 1
1.3-b	M1	300	Backwards 1	2.3-b	M2	300	Backwards 1
1.3-c	M1	300	Forward 2	2.3-c	M2	300	Forward 2

Figure 22 show the results of shear stress applied horizontally and in both directions over the prepared molds of soils. The shear stress was applied with two forward and one backwards motion. Each mold had a testing time of approximately 3 days, that includes saturation, consolidation and direct shear cut. All of the test were running at the same velocity of 0.021 mm/min to reach a 15 mm displacement at the 12-hour mark. These conditions would allow the test to run slow enough that will allow only soil shear resistance, and long enough to find the residual shear strength.

In regards to the shear strength of each sample, the graph displays a tendency to a residual value, in most cases. The tests that were running with the two lowest vertical forces (tests 1.1; 1.2; 2.1 and 2.2) had little to no problems during the experiment. When the vertical load was at 300 kPa both samples encountered some problems. In particular, the ones with the most vertical load had problems reaching the estimated displacement. After the 12-hour mark test 1.3-c would reach a displacement of 12 mm, but fortunately that was enough to see how the shear

strength tends to a residual value of 171.6 kPa. This situation was also present, at a lower degree, in the 2.2-c test, where the sample reached around 13.5 mm on the second forward motion after the 12-hour mark.

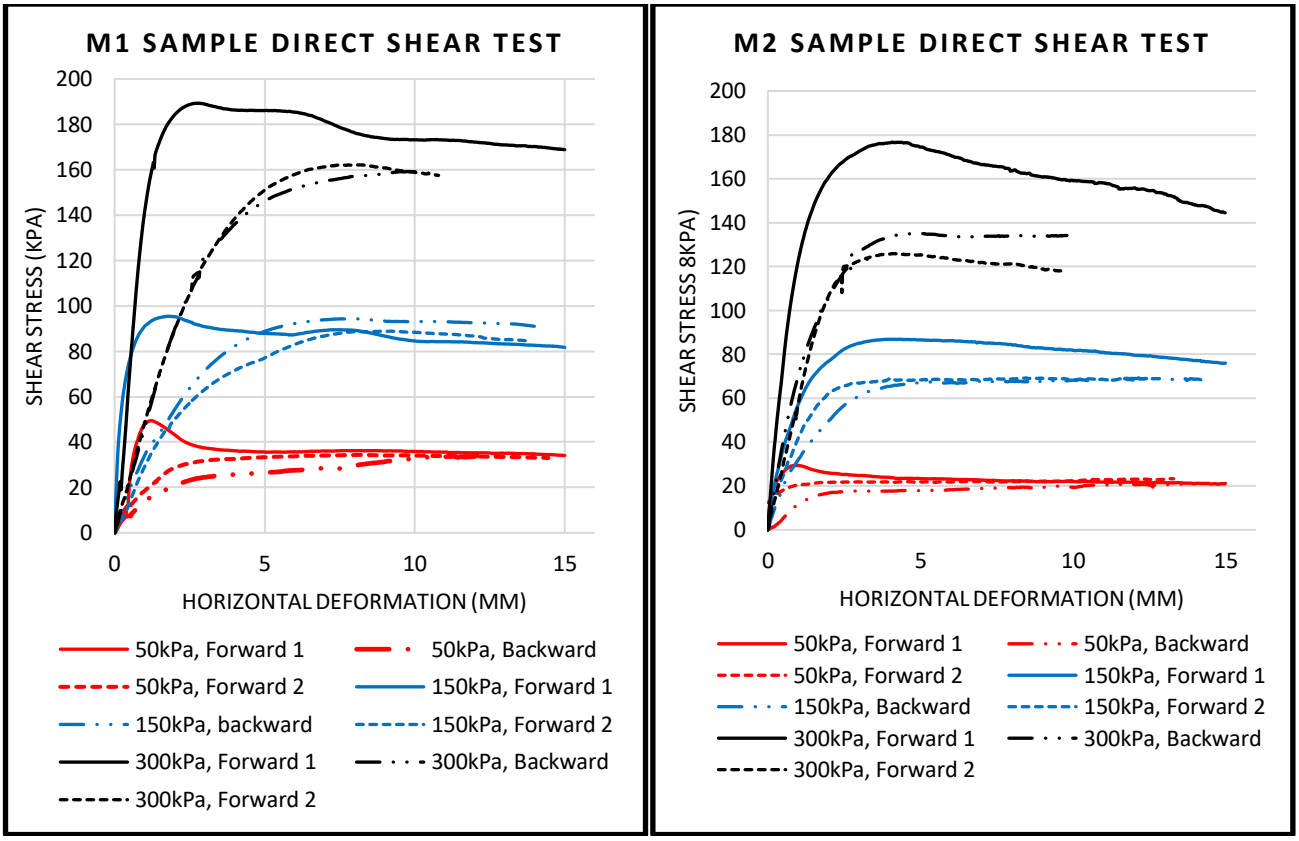

Figure 22: Direct shear results for Soil M1 and M2.

During the direct shear test no samples had any visible problems while the first forward shear stress was applied, all of them would reach the 15 mm displacement. For the first backwards and the second forward motion the porous plate would shift from a horizontal to tilted position. This problem affects how the vertical load is applied and it will generate horizontal forces that most likely disturb the shear stress acting on the shear box, as seen on figure 23.

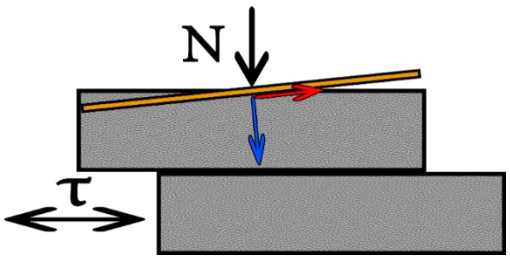

Figure 23: Representation of tilted porous plate and associated forces

The vertical load will not be uniformly distributed over the surface of the sample and this should be the cause of altered results.

By analyzing the results on figure 22, there is a similar behavior for all tests. All samples have a maximum value of resistance that drops to an almost constant magnitude, at that point the soil has reached its residual shear

strength. This behavior is proper for tests done with dense sands and over consolidated clay, this can be observed in the example graph in figure 24 (Dafalla, 2012).

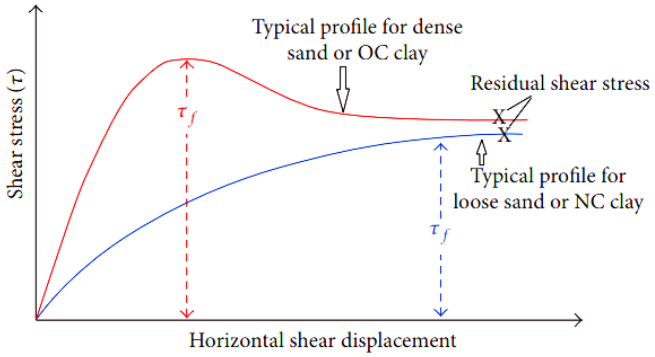

Figure 24: Typical shear stress versus horizontal shear displacement(OC stands for over consolidated and NC stands for normally consolidated). (Dafalla, 2012)

The results match what was expected from this test. There is at first the dense soil which has been compacted which has a higher shear resistance. Once the link between the particles is broken it is in a much looser state where it will never be able to obtain the maximum strength that it once had, only being able to reach the residual resistance.

Table 8: Maximum and residual shear resistance for both samples

	Vertical stress (kPa)	τ Max (kPa)	τ Residual (kPa)
M1	50	49.17	37.1
	150	95.36	86.2
	300	189.2	171.8
M2	50	29.36	28.9
	150	86.33	77.66
	300	176.6	154.88

Luckily in each test it can be observed the tendency of the soil, being in both dense and loose state, to approach its residual value.

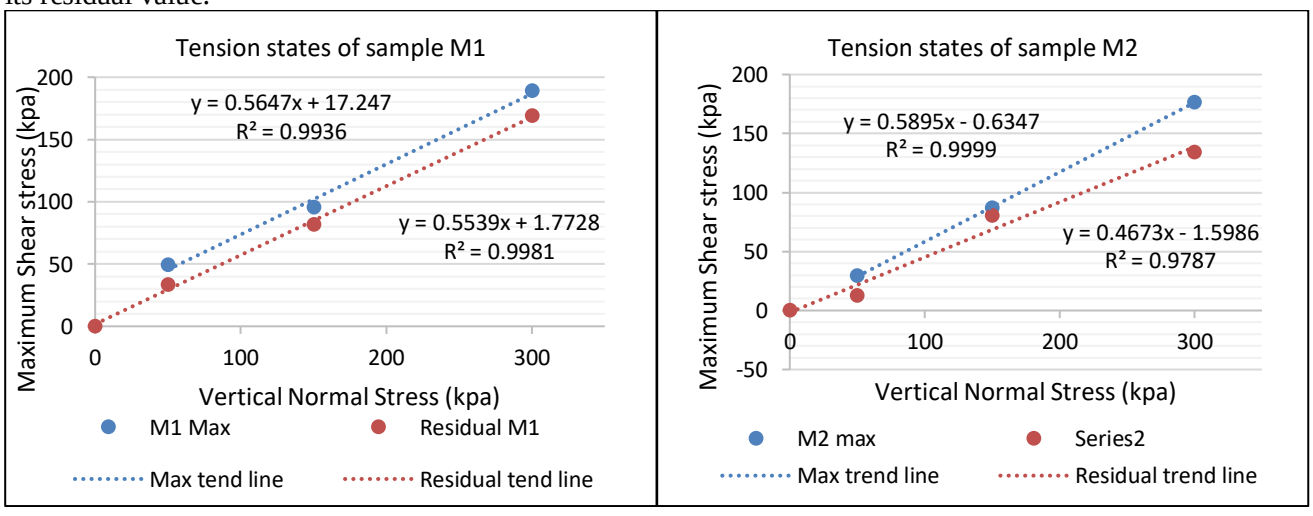

Figure 25: Tension states of soil M1 and M2

Table 9: Results for max and residual states of the soil

element	M1 max	M1 residual
Ø (rad)	0,5647	0,5539
Ø (°)	32,35	31,74
C (kPa)	17,028	0

element	M2 max	M2 residual
Ø (rad)	0,5895	0,4673
Ø (°)	33,78	26,77
C (kPa)	17,028	0

3.2 Field tests

This section contains procedures that were performed at the location of the embankment, such as topography and the geophysical analysis. These procedures were done to characterize the embankments shape and slope as well as its load-bearing capability through a shear-wave velocity analysis.

3.2.1 Topography

The slope analyzed had a very irregular form due to it sliding and failing over time, also the weather conditions would aggravate the structure even more. For the elaboration of a digital embankment model an approximation to the geometry of the actual structure was required. Figure 26 displays top view of the embankment after a radial survey of the slope was done. Several points where registered over the embankment at different heights, a total station was used to gather the information that was afterwards processed on Microsoft Excel, later to be presented through the use of AutoCAD. In the following image red-like colors represent the lower part of the embankment while the crest is shown as green, blue and purple.

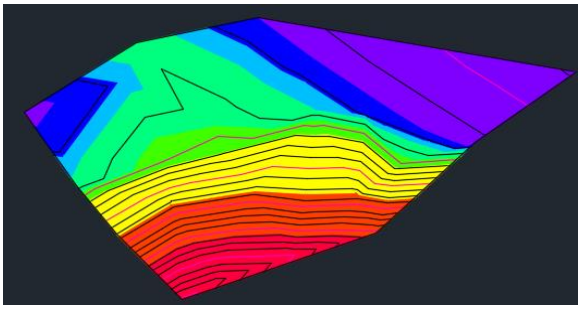

Figure 26: Topographic representation using AutoCAD

The average value of the slope was obtained using a ponderation of the minimum and maximum slope and the area occupied. The process is all summarized in table 10 where the average slope was around 58%.

Table 10: Minimum and maximum ponderation of slope values

Section	Min Slope (%)	Max Slope (%)	Area (%)	Min ponderation	Max ponderation
1	5,92%	8,35%	0	0	0
2	8,35%	9,52%	0	0	0
3	9,52%	21,34%	0	0	0
4	21,34%	40,98%	12,95	2,76	5,31
5	40,98%	55,42%	22,83	9,36	12,65
6	55,42%	64,75%	20,04	11,11	12,97
7	64,75%	70,21%	23,50	15,22	16,50
8	70,21%	79,36%	20,68	14,52	16,41
	34,56%	43,74%	100,00	52,96	63,84
				Average	58,40

3.2.2 Geophysical analysis

Using a MASW was used to obtain measurements of the shear-wave velocity along the crest of the embankment and through the middle from crest to the lowest part that was accessible. Figure 27 displays the variation of velocities through the mass of soil as far as 60 meters of depth. It's possible to make out how the stratigraphy may be organized below the surface without the need of drilling holes.

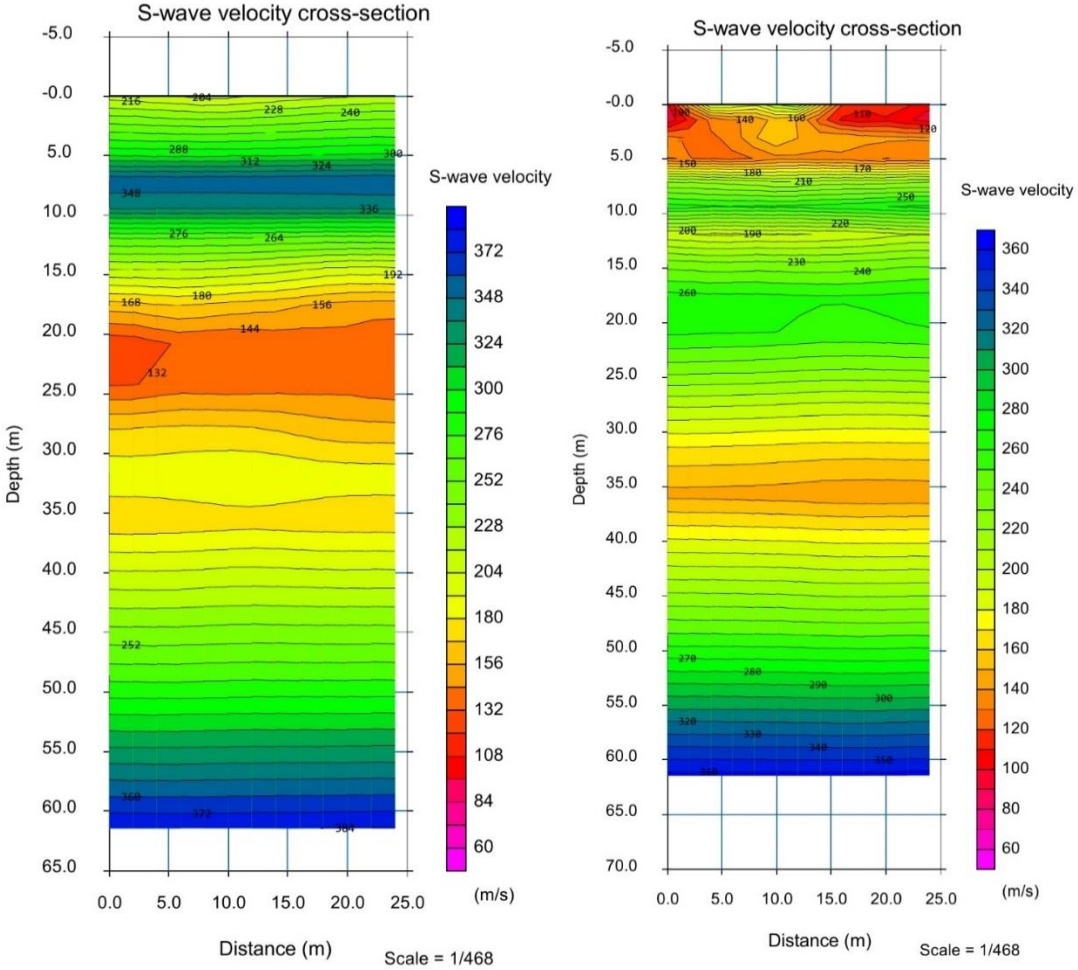

Figure 27: Longitudinal and transversal Velocity Cross-Sections, without using filters

The Vs30 for the Longitudinal line of this test was calculated to be equal to 209.4 m/s and for the transversal line it was equal to 202.1 m/s.

The results of this analysis are the following, in table 11 Vs30 velocity will be determined using formula (10):

Table 11: Vs30 for Tomé soil

Transversal			
Stratum	Velocity (m/s)	Width (m)	hi/Vs-i
1	100	2.5	0.025
2	170	2.5	0.014705882
3	230	25	0.108695652
Vs30 [m/s] =			202.1542439

From the "REGULATION, THAT FIXES THE SEISMIC DESIGN OF BUILDINGS AND REPEALS. DECREE No. 117, OF 2010", it is possible to classify the soil under category of a D (medium dense soil) type of soil. Table 12 provides the classification for the Vs30 values.

Table 12: Seismic classification of the foundation terrain

Soil Type		Vs30 (m/s)	RQD	qu (MPa)	(N1) (strikes/foot)	Su (Mpa)
A	Boulder, cemented soil	≥ 900	≥ 50%	≥ 10 (εqu≤2%)		
B	Soft rock or fractured, very dense soil or firm	≥ 500		≥ 0.40 (εqu≤2%)	≥ 50	
C	Dense soil or firm	≥ 350		≥ 0.30 (εqu≤2%)	≥ 40	
D	Medium dense soil, or firm	≥ 180			≥ 30	≥ 0.05
E	Soil of a medium compacity or consistance	< 180			≥ 20	< 0.05
F	Special soils	*	*	*	*	*

Where:

N1 = Standard penetration index normalized by confining pressure of 0.1 MPa.Apllied only to soils that are classified as sands.
RQD = Rock Quality Designation. According to ASTM D 6032
qu = Resistance to simple compression of the soil
Su = Resistance to non-drained soil cutting.

3.3 General equilibrium model

The following results are for 3 positions of the phreatic level: high, medium and low. Figure 28 displays the variation of friction angle and cohesion on the abscissa axis and ordinate axis respectfully.

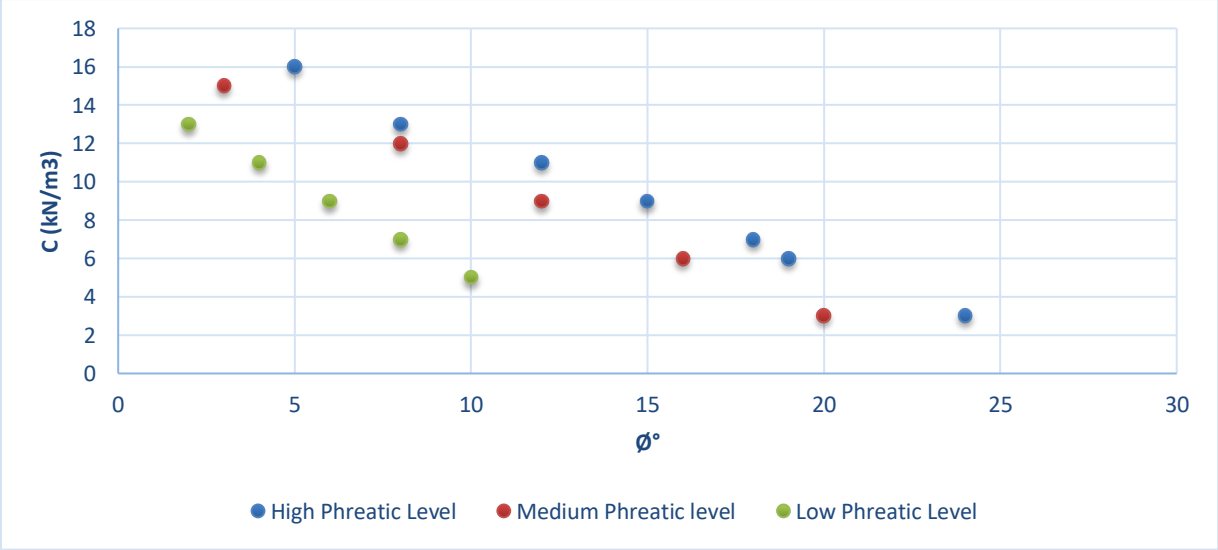

Figure 28: Pair values of the internal friction angle and cohesion for FOS=1

These results are for the embankment's soil sample and every point in the graph represents a generated critical slip surface. Both properties change to maintain the FOS at 1, they are inversely proportional magnitudes and each one will contribute to the soils resisting strength. When the Phreatic level is lowest, the variations between friction angle and cohesion are constant. At higher levels of water, the cohesion changes are having a greater effect on the resistance than the friction angle.

Regulations must be carried out to assure a good interlocking between particles by compaction to have a greater value of friction angle. The cohesion is an important factor to the soils strength that can be controlled with well-known properties. Regmi (2015) states that "Cohesion depends on bonding of fine-grained particles (i.e., clays and fine silts), physical properties of soils such as soil-moisture content, grain-size distribution and relative density, and root strength. Increasing soil moisture reduces soil cohesion and thus, soil strength". It is possible during embankment constructions to manipulate the soil properties that will allow higher values of cohesion and friction angle. This will make it possible to have more stable construction and not have situation like the one in this investigation.

4 CONCLUSIONS –RECOMMENDATION

As a first conclusion it is most likely that soil M1 required a better compaction procedure. The Moisture-density relation and the Atterberg limit tests suggest that both samples, embankment and surroundings, should act in a similar way under the presence of water. Although sample M1 can become unstable with a lower amount of moisture. Rainstorms over Tomé city, the study zone, have produced structural damage and overflowing of rivers, like the scenario that took place on May 29th, 2018. Due to the fact that events of this magnitude can affect the zone but the surrounding soil structures are unaffected, there is a high chance that moisture has penetrated through the embankment changing its behavior.

Some results of the direct shear test are just approximations observed in the graph for the test where the final motion was not able to finish properly. The results were more successful for tests: 1.1; 1.2; 1.3; 2.1; and 2.2, where test number 2.3 was the least successful. On the last test mention it may have been possible to find an even lower value of residual shear strength, the graph never was able to stabilize and the magnitude was still going down. This would mean that the value obtained from this last test may be discarded and further on the procedure could be replicated at a lower speed and with a higher displacement target to acquire an improved result.

For the shear resisting properties present in the embankment, cohesion and friction angle. It is necessary to control them during the construction process, small changes in these factors can result in large critical slip surfaces. Figure 14 displays an example of a slip surface with a critical FOS that can occupy up to half of the concrete road over the soil structure. Similar to the actual scenario shown in this article, where there are visible cracks over the concrete road up to almost half of its width.

5 REFERENCES

Ministerio de Vivienda y Urbanismo - Minvu. (2018). *CÓDIGO DE NORMAS Y ESPECIFICACIONES TÉCNICAS DE OBRAS DE PAVIMENTACIÓN.* Santiago.

Acedo, J. F. (2000). *ORDEN CIRCULAR 326/00 SOBRE GEOTECNIA VIAL EN LO REFERENTE A MATERIALES PARA LA CONSTRUCCIÓN DE EXPLANACIONES Y DRENAJES.* Madrid.

Chok, Y. H. (2008). *MODELLING THE EFFECTO OF SOIL VARIABILITY AND VEGETATION ON THE STABILITY OF NATURAL SLOPES.*

Dafalla, M. A. (2012). *Effects of Clay and Moisture Content on Direct Shear Tests for.* Saudi Arabia.

Dirección de Vialidad. (2010). *Mabual de carreteras - Especificaciones y métodos de muestreo, ensaye y control.*

EXCAVACIONES RB. (2016). Retrieved from http://excavacionesrb.com/

F. Craig, R. (2004). *Craigs Soil Mechanics.* Canada.

FHWA. (2001). *Soil Slope and Embankment Design Reference.*

GEO-SLOPE International. (2012). *Stability Modeling with SLOPE/W.* Alberta.

Gonzales de Vallejos, L. (2002). *Ingeniería Geológica.* Madrid.

Han, J. (2015). *Principles and Practices of Ground Improvement.* Canada.

Hernvall, H. (2017). *Clay slopes and their stability: An evaluation of different methods.* Gothenburg.

Jeria H., R. (2018). *Curso Laboratorista Vial Clase C.*

Jones, C. (2002). *Guide to reinforced fill structure and slope design.*

Keller, G., & Sherar, J. (2003). *Low Volume Roads Engineering.* California.

Mason, D. (2017). *Performance of road networks in the 2016 Kaikōura earthquake: observations on ground damage and outage effects.* Napier.

MINISTRY OF HOUSING AND URBANISM. (2011). *REGULATION THAT FIXES THE SEISMIC DESIGN OF BUILDINGS AND REPEALS.*

MOPU direccion general de carreteras. (n.d.). *Recomendacions para el control de calidad en obras de carreteras.*

Patil, P., Mena, I., Goski, S., & Urs, Y. (2016). *Soil Reinforcement Techniques.*

RAWAT, S. (2017). *Testing and modeling of soil - nailed slopes.* India.

Ruiz Uribe, J. F. (2007). *CONTROL DE MAQUINARIA CON TECNOLOGIA GPS.* Valdivia.

Salem Valderrama, I. S. (2016). *Estudio sobre la relevancia de la ejecución de sondajes exploratorios como complemento de las mediciones geofísicas de ondas superficiales.* Santiago.

TAPIA, R. P. (2004). *MAPA DE RECONOCIMIENTO DE SUELOS DE LA VIII REGIÓN.* Santiago.

Terzaghi, K. (1996). *Soil Mechanics in Engineering Practice.* Canada.

(n.d.).*The Sideling Hill Road Cut.* Maryland.

Universidad de Cantabria. (2010). *Geotecnia I (2010) .*

UNIVERSIDAD DE CONCEPCIÓN. (2008). *Mapa Geológico del Sector Menque Concepción.*

USDA. (2015). *National Engineering Handbook, Chapter 8 Earthfill and Rockfill.*